Journal of Porphyrins and Phthalocyanines
J. Porphyrins Phthalocyanines 2012; **16**: 163–174
DOI: 10.1142/S1088424612004495

Published at http://www.worldscinet.com/jpp/

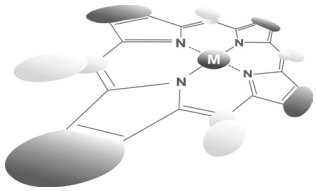

Tetra and octa(2,6-di-*iso*-propylphenoxy)-substituted phthalocyanines: a comparative study among their photophysicochemical properties

Ahmad Tuhl[a◊], Wadzanai Chidawanayika[b], Hamada Mohamed Ibrahim[a], Nouria Al-Awadi[a], Christian Litwinski[b], Tebello Nyokong[b◊], Haider Behbehani[a], Hacene Manaa[c] and Saad Makhseed*[a]

[a] *Department of Chemistry, Kuwait University, P.O. Box 5969, Safat 13060, Kuwait*
[b] *Department of Chemistry, Rhodes University, Grahamstown 6140, South Africa*
[c] *Department of Physics, Kuwait University, P.O. Box 5969, Safat 13060, Kuwait*

Received 10 September 2011
Accepted 23 October 2011

ABSTRACT: This work reports on the synthesis of novel metal free, zinc, aluminum, gallium and indium tetra and octa (2,6-di-*iso*-propylphenoxy)-substituted phthalocyanine derivatives. UV-visible and ^{1}H NMR analyses confirm that a non-planar conformation, adapted by the phenoxy substituents due to steric interaction in both derivative series, perfectly discourage cofacial aggregation. Fluorescence quantum yields vary as a function of the number of substituents on the ring periphery, while the fluorescence lifetimes display no distinct trend. Triplet quantum yields are significantly larger for the tetra 2,6-di-*iso*-propylphenoxy-substituted derivatives relative to their corresponding octa-substituted species. However there was no overall trend in the triplet lifetime values. For almost all of the phthalocyanine derivatives, singlet oxygen was produced with relatively good quantum yields. This study explores the possibility of fine-tuning their physicochemical properties by simple structural modification.

KEYWORDS: di-*iso*-propylphenoxy, phthalocyanine, photochemistry, photophysics.

INTRODUCTION

Phthalocyanines (Pcs) and derivatives thereof show potential as photosensitizers for many applications including in non-linear optics and photodynamic therapy (PDT) [1–8]. For these applications, large triplet state yield and long triplet state lifetimes are required.

With their π-conjugated planar organic structure, Pcs interact strongly with light over most of the visible spectrum. Diversification of the phthalocyanine by substitution at the ring periphery, axial position and central metal atom could alter the solubility, electronic absorption characteristics and photosensitizing behavior of Pcs [9, 10].

MPc derivatives containing diamagnetic non-transition centrals, are photoactive, and are often employed in photosensitization [11–13]. Interest in improving the photophysical properties of the Pc ring system continues to grow rapidly. This has stirred research into examining new Pc compounds whose structures promote good photophysical behavior [14–16]. Therefore this work is focused on the synthesis and subsequent photophysicochemical characterization of novel tetra and octa di-*iso*-propylphenoxy substituted metal free, aluminum, zinc, gallium and indium phthalocyanines. For the di-*iso*-propylphenoxy tetra substituted complexes, the chlorine atom is also present on the periphery of the ring. Halogenated phthalocyanines have been reported to show improved photosensitizer activity for PDT compared to non-halogenated derivatives [17–19]. With the exception of octa-substituted zinc derivative [20, 21] to date there have been no reports on the synthesis of tetra-substituted derivatives. Ameliorating the

◊SPP full member in good standing

*Correspondence to: Saad Makhseed, email: saad.makhseed@ku.edu.kw, tel: +965 24985538, fax: +965 24816482

photosensitizing efficiency of phthalocyanines may also be achieved by the presence of four chlorine atoms on the ring periphery (for complexes **4a**–**8a**), due to the heavy atom effect [22, 23]. Moreover, electron-withdrawing groups (*i.e.* chlorine atoms) are known to increase the photo-oxidative stability, which could impart additional features for such material in PDT and non-linear optical (NLO) applications [24, 25].

The aim is thus to establish the influence of the different metal centers and substitution patterns, with respect to the photophysicochemical properties of the complexes.

RESULTS AND DISCUSSION

Synthesis and characterization

The phthalonitrile precursors (**3a** and **3b**) mono and di-substituted with di-*iso*-propylphenoxy were employed to synthesize the tetra (Scheme 1) and octa (Scheme 2) substituted metal free, aluminum, zinc, indium and gallium phthalocyanines respectively. Phthalonitriles **3a** and **3b** were prepared by the well-known base catalyzed nucleophilic aromatic substitution reaction between 4,5-dichlorophthalonitrile and the anion of the sterically hindered phenol (2,6-di-*iso*-propylphenol) in good yield [26]. Following the metal-ion-mediated reaction procedure, the precursor **3a** undergoes cyclotetramerisation in quinoline using the appropriate metal salt ($AlCl_3$, $GaCl_3$, $InCl_3$ and $Zn(OAc)_2$) with a catalytic amount of 1,8-diazabicyclo[5.4.0]undec-7-ene (DBU) to afford metal-containing derivatives **5a**–**8a** in acceptable yields as a mixture of inseparable structural isomers. Cyclization of **3a** in pentanol with lithium metal (*i.e.* the most routinely followed procedure) to prepare the metal-free phthalocyanine derivative (**4a)** was avoided to protect the peripheral chlorine atoms from the possibility of being displaced by the alkyloxide anion. Therefore, the synthesis of **4a** was best achieved in reasonable yield simply by urea-promoted cyclization of **3a** in quinoline. **4b** was synthesized using the lithium method. Due to the asymmetrical arrangement of the substituents in the periphery of the macrocycle, all **4a**–**8a** products are obtained as a mixture of structural isomers which are highly soluble in most organic solvents *e.g.* dichloromethane (DCM), $CHCl_3$, tetrahydrofuran (THF), toluene and hexane thus facilitating their purification by column chromatography. Each of **4a**–**8a** complexes occurs as a mixture of structural isomers which are difficult to separate these isomers by column chromatography or high performance liquid chromatography (HPLC) technique. The octa-substituted derivatives (**5b**–**8b)** were prepared by following the same procedure used to prepare the tetra 2,6-di-*iso*-propylphenoxy-substituted complexes (**5a**–**8a**). The identity and purity of the prepared complexes were confirmed by ^{1}H NMR, IR, UV-vis spectroscopies, fast atom bombardment (FAB) mass spectroscopy and elemental analysis. All the techniques employed gave further confirmation of the predicted structural configuration of the molecules as detailed in the experimental section.

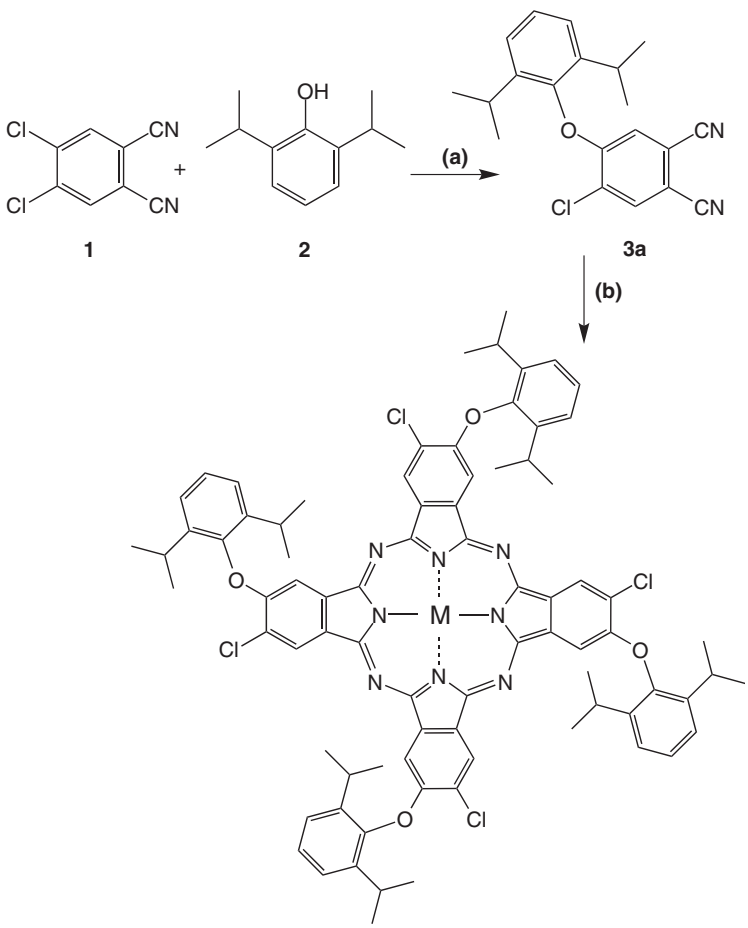

M = H_2 (**4a**); Zn (**5a**); AlCl (**6a**); GaCl (**7a**); InCl (**8a**)

Scheme 1. Synthetic route to tetra-substituted 2,6-di-*iso*-propylphenoxy phthalocyanines **4a**–**8a**. Reagents and conditions: (a) anhydrous K_2CO_3, DMF, 45 °C, 24 h; (b) appropriate metal salt, quinoline, 180 °C, 12 h, inert atmosphere

Structural and self-association characterization using proton NMR

The efficient π–π stacking of disc-like molecules such as phthalocyanines results in aggregation, even in dilute solution, into dimer, trimer and higher oligomers. Such intrinsic behavior can considerably affect their properties (*e.g.* opto-electronic properties) and of course limit their uses in the intended applications such as in the

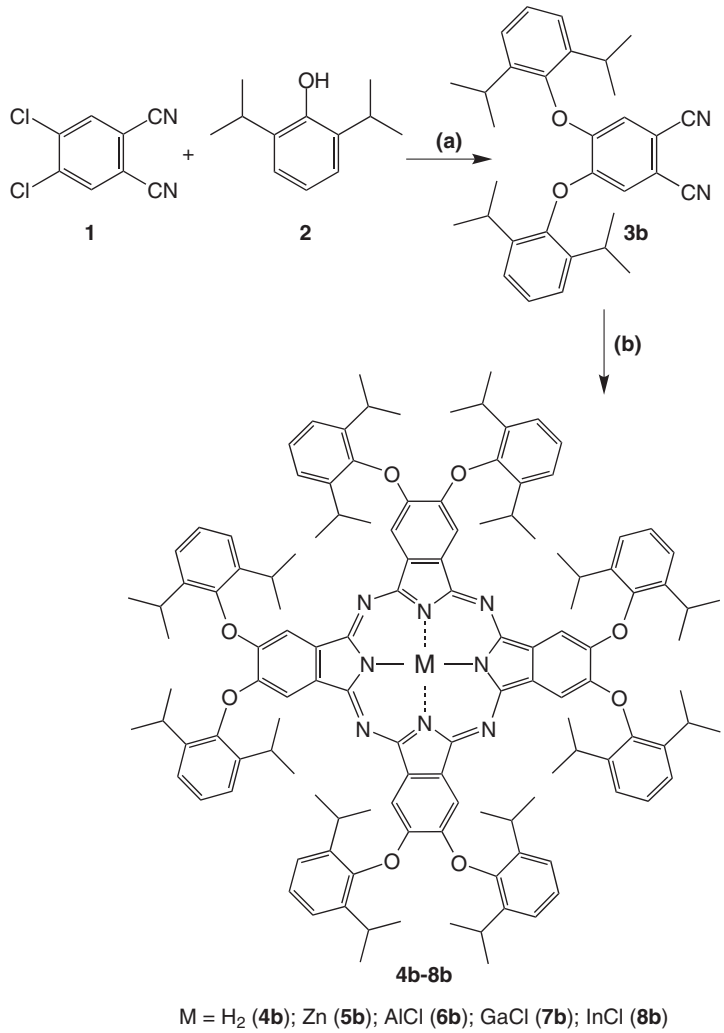

Scheme 2. Synthetic route to octa-substituted 2,6-di-*iso*-propylphenoxy phthalocyanine **4b**–**8b**. Reagents and conditions: (a) anhydrous K_2CO_3, DMF, 80 °C, 24 h; (b) appropriate metal salt, quinoline, 180 °C, 12 h, inert atmosphere

NLO and PDT fields [9, 15, 27–30]. UV-vis [31–33] and NMR [34] spectroscopic techniques were, therefore, used to evaluate the aggregation behavior of the target complexes.

It was noted previously that the ^{1}H NMR analyses of the disubstituted phthalonitrile **3b** demonstrated that the phenyl rings bearing two *iso*-propyl groups are forced out of the plane of the benzene-containing dicarbonitriles due to the bulkiness exerted by the presence of two isopropyl groups [21]. This informative conformation was clearly detected by the ^{1}H NMR spectrum which displays a doublet of doublets for the methyl groups at 298 K due to the frozen rotation about the aryl-oxygen bonds on the NMR time-scale as shown in Fig. 1. Surprisingly, the ^{1}H NMR spectra of the mono-substituted phthalonitrile **3a** at 298 K shows the same conformation adapted by the phenoxy groups in the derived phthalonitrile **3b** and correspondingly displays two environments for the methyl hydrogens of the *iso*-propyl groups. Such findings impart that the chlorine atom next to the bulky phenoxy substituent in **3a** is big enough to introduce steric hindrance which prevents rotation around the aryl ether linkage and consequently forces the phenoxy substituent out of the plane of the target molecule, where the *iso*-propyl groups adopt a configuration, leading to two different methyl hydrogen environments. Thus, the resulting conformational arrangement adopted by the substituents in **3a** would interestingly ensure that cofacial self-association of the derived Pc cores is prohibited. Variable-temperature studies using NMR techniques showed that the coalescence of the methyl hydrogen peaks for **3b** and **3a** occurs at 308 K and 348 K, respectively, corresponding to a free energy of activation (ΔG^*) of 65.8 and 75.8 KJ.mol^{-1}, respectively (Figs 1 and 2 for 348 K, Table 1).

This energy barrier difference between the phthalonitriles under investigation can be attributed to the greater steric effect imposed by the chlorine atom as a result of interaction with the mono phenoxy substituent in **3a,** in comparison with the effect of the second phenoxy substituent containing **3b** which provides more freedom of movement for the conformational processes required for methyl interchange.

The intrinsic tendency of phthalocyanine molecules toward aggregation can usually result in a poor quality NMR spectrum characterized by the broadening and up field shift of proton peaks [29, 35]. Therefore, we use the NMR technique along with UV-vis spectroscopy to evaluate the self-association behavior of

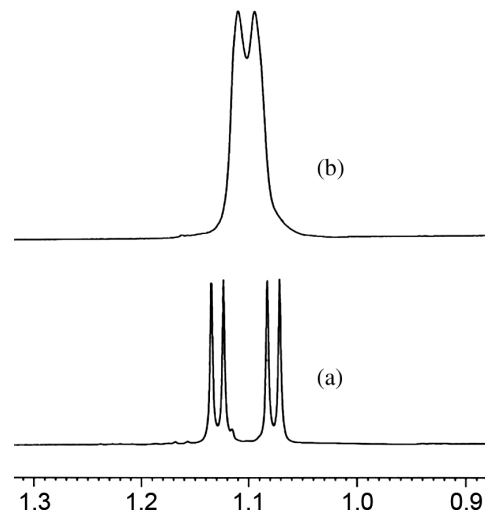

Fig. 1. The ^{1}H NMR spectra of the aliphatic region (methyl groups of the di-*iso*-propyl units) of 4-chloro-5-(2,6-di-*iso*-propylphenoxy) phthalonitrile (**3a**) at different temperatures in DMSO-d_6 (a) 298 K and (b) 348 K

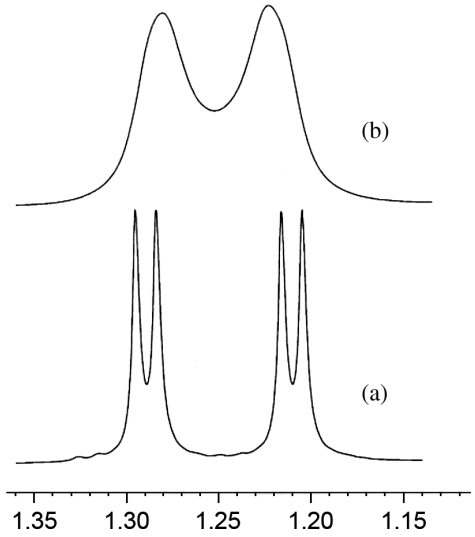

Fig. 2. The ^{1}H NMR spectra of the aliphatic region (methyl groups of the di-*iso*-propyl units) of 4,5-bis-(2,6-di-*iso*-propylphenoxy) phthalonitrile **(3b)** at different temperatures in $CDCl_3$ (a) 273 K and (b) 308 K

Table 1. Activation energy calculations of 4-chloro-5-(2,6-di-*iso*-propylphenoxy)phthalonitrile **(3a)** in comparison with the 4,5-bis-(2,6-di-*iso*-propylphenoxy)phthalonitrile **(3b)**

Materials	Tc, K	Δυ, Hz	ΔG*, kJ.mole
3a	348	31.8	75.8
3b	308	45.6	65.8

the prepared complexes. The NMR spectra for **4a**–**8a** the prepared complexes recorded in $CDCl_3$ were almost identical and show complicated and overlapped resonant peaks which were difficult to assign due to the mixture of isomers characteristic of the prepared Pcs. Nonetheless, integration of the peaks correctly corresponded to the expected total number of protons for each complex, thus confirming the relative purity of the complexes which is supported by the elemental and mass spectrometry analysis. For example, the NMR spectrum of **5a** consists of two distinct aliphatic and one aromatic region: several overlapped doublet peaks at ε: 1.10–1.60 ppm belonging to the methyl protons, four septet peaks in the range of ε: 3.21–4.21 ppm attributed to the methylene protons and complicated multiplet peaks at ε: 7.39–9.05 ppm related to the aromatic protons. The qualities of ^{1}H NMR spectra of **4a**–**8a** complexes remain unchanged even after the addition of trace amount of pyridine-D_5 into the ^{1}NMR sample solution. Although, the overlapped aromatic peaks are separated from each other due to the chemical shift induced by pyridine-D_5. In addition, all octa-substituted derivatives (**4b**–**8b**) show very simple and well resolved spectra with sharp peaks in both aromatic and aliphatic regions due to their high symmetry and the total absence of aggregation. Indeed, the defined signal patterns, including the absence of both broadening and chemical shifts of the prepared complexes, were essentially independent of the concentration and the appearance of the spectra remained unchanged over the concentration range between 1×10^{-4} and 1×10^{-2} M at room temperature [35]. Such behavior can be attributed to the position adopted by the bulky phenoxy substituents relative to the Pc core that successfully prevents efficient π–π stacking of the macrocycle units.

Ground state electronic absorption and fluorescence spectra

Figures 3 and 4 show the ground state electronic absorption spectra pertaining to the metal free, aluminum, zinc, indium and gallium tetra-di-*iso*-propylphenoxy (**4a**–**8a**) and octa-di-*iso*-propylphenoxy (**4b**–**8b**) phthalocyanines, respectively in DMF. All spectra remain monomeric up to 2×10^{-5} M (Beer–Lambert law was obeyed below these concentrations) and exhibit sharp bands typical of non-aggregated species. The presence of axial ligands associated with the aluminum, indium and gallium central metal atoms, is particularly useful in preventing aggregation. Axial ligands in this position restrict the stacking interaction of multiple MPc molecules, often reflected by broad and blue shifted absorption bands in the UV-vis spectrum [36–38].

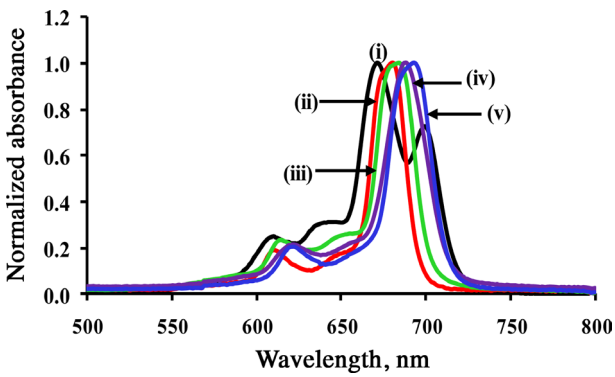

Fig. 3. Normalized ground state electronic absorption spectra of (i) **4a**, (ii) **5a**, (iii) **6a**, (iv) **7a** and (v) **8a** in DMF

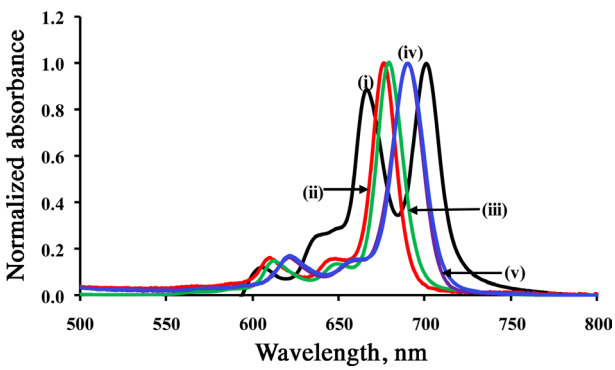

Fig. 4. Normalized ground state electronic absorption spectra of (i) **4b**, (ii) **5b**, (iii) **6b**, (iv) **7b** and (v) **8b** in DMF

Complexes **5a**, **6a** and **8a** show a slight red shift in the Q-band maxima relative to the corresponding octa-substituted complexes **5b**, **6b** and **8b** proving that the highest occupied molecular orbital (HOMO) to lowest unoccupied molecular orbital (LUMO) energy gap is reduced upon the introduction of chlorine atoms [24, 25, 39]. As anticipated, the electronic spectra of the tetra and octa (2,6-di-*iso*-propylphenoxy)-substituted phthalocyanine complexes showed monomeric behavior in solution using different organic solvents (CH_2Cl_2, $CHCl_3$, THF and DMF) as confirmed by the position and the appearance of intense Q-band peaks. The spectrum in less coordinating solvents such as chloroform was similar to that in DMF (Fig. 3) which is typical of non-aggregated species belonging to D_{4h} symmetry. However, the monomeric Q-band position of **5b** is blue shifted relative to that of **5a** proving that the HOMO-LUMO energy gap is reduced upon the introduction of chlorine atoms. This marginal red shift, caused by chlorine atoms, is consistent with the concept that the chlorine atoms are participating in the π-electron system of the Pc complexes and act as electron donor substituents by mesomeric effects which may provoke noticeable changes in photoelectric behavior [22, 23, 40].

Similarly, a shift to longer wavelengths with an increase in central metal size is due to an increase in electron density, where the order of Q-band positions is $Zn^{2+} < Al^{3+} < Ga^{3+} < In^{3+}$ (Table 2) for the **4a**–**8a** complexes. For the octa-substituted complexes the trend is the same as for the **4a**–**8a** complexes, except **7b** and **8b** have the same wavelength. The notable red shift for InPc derivatives may be attributed either to distortion of the macrocycle in which the indium (*i.e.* the largest size among the transition metals used in this study) is out of the π-planar system creating a non-planar system or weakness of the coordination M–N bond [41], due to a decrease in electronegativity on going from Al to In, which leads to higher π-electron density of the system and therefore the lower energy gap between HOMO and LUMO is consequently observed.

With the exception of InPc and GaPc derivatives, all the molecules showed fluorescence emission and excitation spectra typical of phthalocyanines, where the excitation is similar to absorption and both are mirror images of the fluorescence emission, Fig. 5 for **6a** in DMF. The behavior of InPc and GaPc derivatives could be related to their size which may result in changes in symmetry upon excitation. A flexible σ-bond connecting the phenoxy ring to the local MPc ring may allow for photoinduced twisting which distorts the MPc molecule. Stokes shifts were typical of MPc derivatives [11].

Photophysicochemical parameters

Fluorescence quantum yields and lifetimes. Fluorescence quantum yields reflect the fraction of absorbing molecules, excited to the singlet state and subsequently deactivated *via* radiative means. Thus the quantum yield is a ratio of the number of photons emitted relative to the number of photons absorbed [42]. Variations in fluorescence quantum yield values have been explained by a number of prevailing conditions including temperature, molecular structure and solvent parameters (polarity, viscosity, and refractive index). In this case, considering molecules with the same number of substituents, there is a trend towards lower quantum yields with increase in size of central metal for the **4a**–**8a** species *i.e.* Zn(**5a**) > Ga(**7a**) > In(**8a**) (Table 3) and similarly for the octa-di-*iso*-propyl-substituted species. Such behavior is expected on the grounds of spin-orbit coupling induced by the respective central metal ions. In^{3+} being the largest central metal ion induces a greater

Table 2. Absorption, fluorescence emission and fluorescence excitation spectral data for MPc complexes **4a**–**8a** and **4b**–**8b** and **ZnPc** in DMF

MPc	Q-band λ_{max}, nm	Log ε	Emission λ_{max}, nm	Excitation[a] λ_{max}, nm	Stoke's Shift, nm
ZnPc	669	5.37	685	669	16
4a	671, 700	5.21	707	671, 700	7
5a	680	5.35	697	677	20
6a	683	5.29	696	683	13
7a	688	5.27	702	692	10
8a	693	5.21	712	704	8
4b	667, 701	5.30	709	667, 703	6
5b	675	5.57	693	676	17
6b	679	5.48	697	679	8
7b	690	5.43	710	703	7
8b	690	5.38	713	705	8

[a] Excitation at 580 nm for MPc complexes.

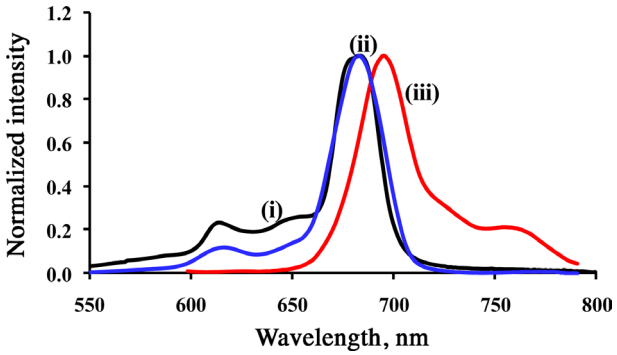

Fig. 5. Normalized ground state electronic absorption (i), fluorescence emission (ii) and fluorescence excitation (iii) of **6a** in DMF

effect, in terms of spin-orbit coupling, thereby increasing the likelihood of the spin-forbidden intersystem crossing (ISC) process to populate the triplet state and an attendant decrease in the spin-allowed fluorescence. Aluminum serves as an exception, due to its small size, with fluorescence quantum yields higher than the Zn metalated species (Table 3). The effect of introducing eight di-*iso*-propylphenoxy substituents to the Pc ring periphery is insignificant in terms of quantum yield values, relative to the tetra 2,6-di-*iso*-propylphenoxy-substituted derivatives (Table 3). However, **6b** gives higher yields relative to the tetra 2,6-di-*iso*-propylphenoxy-substituted derivative, **6a**. This may be in relation to the presence of the chloro-substituent groups in **6a** which have a greater effect, in this case, in terms of deactivation of molecules in the excited singlet *via* non-radiative means such as ISC rather than by fluorescence, as a result of the heavy atom effect.

The fluorescence lifetime gives an indication of how much time the molecule spends in the excited state prior to relaxation back to the ground state. Metallophthalocyanines decay with mono-exponential behavior with fluorescence lifetimes that range between 1–10 ns [43–45]. All phthalocyanines, in this study, exhibit mono-exponential decay kinetic behavior typical of monomeric phthalocyanine species as shown by a typical fluorescence decay curve for **7b** in Fig. 6. The data in Table 3 shows minimal variation with respect to the number of substituents; however a change in central metal is more significant. A similar effect to the fluorescence quantum yields is observed for the most part for fluorescence lifetimes, where the presence of large central metals such as Ga and In experience shortened lifetimes as a consequence of the heavy atom mediated effect. This has also been reported previously for Ga and In derivatives [15, 16]. As with fluorescence quantum yields, the aluminum derivatives **6a** and **6b** deviate from typical behavior to give fluorescence lifetimes higher than those of a corresponding Pc substituted with larger central metal atoms *i.e.* Zn^{2+}, Ga^{3+} and In^{3+}. Aluminum Pcs generally tend to exhibit elevated fluorescence yields [41, 44, 46–48] due to the small size of Al.

Triplet quantum yields and lifetimes. The spin forbidden process of intersystem crossing to populate the triplet-excited state is a result of spin-orbit coupling. Phthalocyanine species that encounter the strongest spin-orbit coupling effects are often accompanied by high triplet quantum yields (Φ_T) which give a measure of the fraction of absorbing molecules that undergo intersystem crossing to the triplet excited state. The Φ_T and triplet lifetimes (τ_T) pertaining to the molecules explored in this work are shown in Table 3. The order of variance, with respect to the octa-substituted derivatives, is consistent with the strengths of induced spin-orbit coupling in the complexes, *i.e.* species metalated with In^{3+} show the highest Φ_T values with the lowest data occurring for the Zn species, although aluminum was expected to give lower values due to its size. For the **4a**–**8a** complexes

Table 3. Photophysicochemical parameters of MPc complexes **4a**–**8a** and **4b**–**8b** and **ZnPc** in DMF

MPc	Φ_F	Φ_T	Φ_{IC}	Φ_Δ	S_Δ	τ_F, ns (±0.04)	τ_T, μs
ZnPc	0.17[54]	0.58[54]	0.25	0.56 [57]	0.97	3.14	330 [58]
4a	0.12	0.83 (700 nm)	0.05	0.52	0.63	3.69	17
5a	0.12	0.81	0.07	0.58	0.72	2.87	69
6a	0.14	0.85	0.01	0.25	0.30	5.52	12
7a	0.07	0.81	0.12	0.35	0.43	3.86	13
8a	0.02	0.77	0.21	0.56	0.73	2.17	19
4b	0.12	0.87 (702 nm)	0.01	0.53	0.56	5.52	10
5b	0.12	0.32	0.56	0.26	0.81	3.00	15
6b	0.24	0.40	0.64	0.36	0.90	5.88	17
7b	0.09	0.51	0.40	0.45	0.88	3.53	6
8b	0.01	0.67	0.32	0.42	0.63	2.76	13

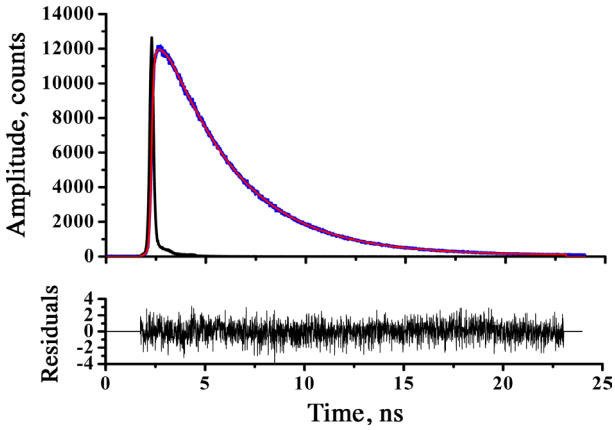

Fig. 6. Fluorescence decay curve of **7b** (red) and instrument response function (IRF, black) in DMF

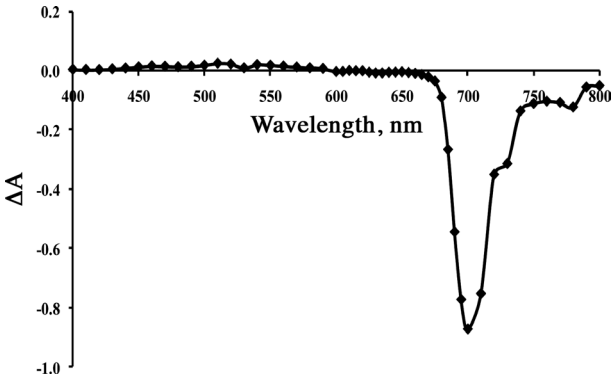

Fig. 7. Transient absorption spectrum of **7a** in DMF (concentration = 1.34×10^{-5} M)

there seems to be minimal effect with increase in size of the central metal. Interestingly the presence of eight 2,6-di-*iso*-propylphenoxy ring substituents gave reduced Φ_T values suggesting that an increase in substituent groups brings about a quenching effect. Such an effect may be in relation to the "loose bolt effect" [49]. A similar effect has been reported for InPc complexes substituted with large phenoxy substituents [16]. The effect is associated with the loss of energy, through internal conversion, as a result of C–H vibrations [49]. An increase in the number of 2,6-di-*iso*-propylphenoxy groups, from four to eight (tetra to octa), gives rise to an increase in C–H bonds and concomitant increased rate of internal conversion and thus a more pronounced "loose bolt" effect. Worthy of note is the transient absorption spectra of **7a**, as an example, shown in Fig. 7. The figure indicates the appearance of a broadened peak centered near 700 nm whereas the absorption spectrum corresponding to this complex shows a maximum at 688 nm (Table 2). Such changes in optical spectra are often a result of symmetry loss, often depicted by splitting or broadening of bands, following photoexcitation [50]. As stated above, a flexible σ-bond connecting the phenoxy ring to the local MPc ring allows for photoinduced twisting which distorts the MPc molecule and thus gives rise to the changes observed. High values of Φ_T for **4a**–**8a** derivatives could also be due to the presence of a halogen (chlorine atom).

The triplet lifetimes determined for the complexes conform to no particular trend ranging from 10–69 μs (Table 3). Such low lifetimes in DMF are common for phthalocyanines containing a large central metal such as In, Ga and Cd, corresponding to high triplet state quantum yields [15, 16, 50, and 51]. The reason for the low lifetime for the AlPc derivatives is not clear, but could be related to the substituents. Unsubstituted ZnPc has a long lifetime compared to complexes **5a** and **5b**, showing the effects of the substituents.

Singlet oxygen quantum yields. The generation of singlet oxygen ($^1O_2$) is a result of the transfer of energy from a phthalocyanine molecule in the triplet excited state to ground state molecular oxygen ($^3\Sigma_g$). The efficiency with which singlet oxygen is generated is quantified by the singlet oxygen quantum yield (Φ_Δ) which varies as a function of triplet state quantum yield, triplet state lifetime, efficiency of energy transfer (S_Δ), triplet state quenching effect of substituents and the triplet state energy. In essence, large triplet state quantum yields should be accompanied in turn by large singlet oxygen quantum yields as shown in Table 3, where **4a**–**8a** derivatives generally give larger quantum yield values compared to their octa-substituted counterparts. Compounds **6a** and **7a** are exceptions, expressing much lower yields than expected based on their triplet quantum yields. In these complexes, the energy transfer process proves to be slightly less efficient as expressed by S_Δ which is a measure of excitation energy transfer efficiency. However, values near unity, as shown in Table 3 for the octa-substituted derivatives, reflect more efficient energy transfer to produce $^1O_2$ as opposed to MPc complexes modified by tetra-substitution with 2,6-di-*iso*-propylphenoxy.

EXPERIMENTAL

Materials

All solvents including dimethylformamide (DMF), dichloromethane (DCM), and tetrahydrofuran (THF) were of reagent grade and purchased from Aldrich. Any purification required was carried out according to Perrin and Amarego [52].

Thin layer chromatography (TLC) was performed using Polygram sil G/UV 254 TLC plates and visualization was carried out by ultraviolet light at 254 nm and 350 nm. Column chromatography was performed using Merck silica gel 60 of mesh size 0.040–0.063 mm.

2,6-di-*iso*-propylphenol (**2**), 4,5-dichlorophthalonitrile (**1**), diphenylisobenzofuran (DPBF) and 1,8-diazabicyclo [5.4.0]undec-7-ene (DBU) were purchased from established suppliers (Sigma-Aldrich, Merck, TCI Europe). All other reagents were purchased from suppliers and used without further purification.

Instrumentation

IR spectra were recorded on a Perkin Elmer system 2000 FTIR. All absorption spectra were undertaken on a Varian Cary 5 UV-vis spectrometer and fluorescence emission and excitation spectra using a Varian Eclipse spectrofluorimeter. ^{1}H NMR spectra were recorded using a Bruker DPX 400 or BrukerAvance II 600. Elemental Analyses were carried out using a LECO Elemental Analyzer CHNS 932. Mass analyses were obtained using a VG Autospec-Q. DSC analyses were carried out on a Shimadzu DSC-50. FAB mass spectra were obtained using a Micro-Mass Tofspec 2E spectrometer.

Fluorescence lifetimes were measured using a time correlated single photon counting (TCSPC) setup (FluoTime 200, Picoquant GmbH). The excitation source was a diode laser (LDH-P-670 with PDL 800-B, Picoquant GmbH, 670 nm, 20 MHz repetition rate, 44 ps pulse width). Fluorescence was detected under the magic angle with a peltier cooled photomultiplier tube (PMT) (PMA-C 192-N-M, Picoquant) and integrated electronics (PicoHarp 300E, Picoquant GmbH). A monochromator with a spectral width of about 4 nm was used to select the required emission wavelength band. The response function of the system, which was measured with a scattering Ludox solution (DuPont), had a full width at half-maximum (FWHM) of about 300 ps. The ratio of stop to start pulses was kept low (below 0.05) to ensure good statistics. All luminescence decay curves were measured at the maximum of the emission peak. The data was analyzed with the program FluoFit (Picoquant GmbH). The support plane approach was used to estimate the errors of the decay times [42].

A laser flash photolysis system was used for the determination of triplet absorption and decay kinetics. The excitation pulses were produced by a Quanta-Ray Nd: YAG laser (1.5 J/9 ns), pumping a Lambda Physik FL 3002 dye laser (Pyridin 1 in methanol). The analyzing beam source was from a Thermo Oriel 66902 xenon arc lamp, and a KratosLisProjekte MLIS-X3 photomultiplier tube was used as the detector. Signals were recorded with a two-channel 300 MHz digital real-time oscilloscope (Tektronix TDS 3032C); the kinetic curves were averaged over 128 laser pulses.

Photo-irradiations for singlet oxygen determinations were done using a General Electric Quartz line lamp (300 W). A 600 nm glass cut off filter (Schott) and a water filter were used to filter off ultraviolet and infrared radiations respectively. An interference filter (Intor, 700 nm with a band width of 40 nm) was additionally placed in the light path before the sample. The light intensity was measured with a POWER MAX 5100 (Molelectron detector incorporated) power meter and found to be 2.97×10^{16} photons.s^{-1}.

Photophysicochemical parameters

Fluorescence quantum yields (Φ_F) were determined as reported in literature [53] using ZnPc as a standard in DMF (with Φ_F = 0.17 [54]). Similarly triplet quantum yield (Φ_T) values were determined according to literature [55] using ZnPc in DMF as a standard (Φ_T = 0.56 [56].

Fluorescence lifetimes were obtained by deconvolution of the decay curves, obtained by time correlated single photon counting (TCSPC), using the FluoFit Software program (PicoQuant GmbH, Germany). Triplet lifetimes (τ_T) were determined by exponential fitting of the kinetic curves using OriginPro 7.5 software.

Quantum yields of internal conversion (Φ_{IC}) were obtained from Equation 1, which assumes that only the three intrinsic processes fluorescence, intersystem crossing and internal conversion; jointly deactivate the excited singlet state of an MPc molecule.

$$\Phi_{IC} = 1 - (\Phi_F + \Phi_T) \quad (1)$$

The fraction of the excited triplet state quenched by ground state molecular oxygen S_Δ was calculated using Equation 2:

$$S_\Delta = \frac{\Phi_\Delta}{\Phi_T} \quad (2)$$

Singlet oxygen quantum yields

Singlet oxygen quantum yield values (Φ_Δ) values were determined in air using the relative method with DPBF acting as a singlet oxygen chemical quencher in DMF, using Equation 3:

$$\Phi_\Delta = \Phi_T^{Std} \frac{R.I_{abs}^{Std}}{R^{Std}.I_{abs}} \quad (3)$$

where Φ_Δ^{Std} is the singlet oxygen quantum yield for the standard ZnPc (Φ_Δ^{Std} = 0.56 in DMF [57]); R and R^{Std} are the DPBF photobleaching rates in the presence of the respective MPc and standard respectively; I_{abs} and I_{abs}^{Std} are the rates of light absorption by the MPc and standard respectively. The concentration of DPBF was lowered to ~ 3×10^{-5} M for all solutions, to avoid chain reactions [57]. DPBF degradation was monitored at ~417 nm.

Synthesis

4-chloro-5-(2,6-di-*iso*-propylphenoxy)phthalonitrile (3a). To a stirred solution of 4,5-dichlorophthalonitrile (**1**, 1.97 g, 10 mmol) and 2,6-di-*iso*-propylphenol (**2**, 1.8 g, 10 mmol) in dry DMF (150 mL) finely ground anhydrous potassium carbonate (4.8 g, 35 mmol) was added. The reaction mixture was heated at 45 °C under nitrogen for 24 h. On cooling, the reaction mixture was poured into acidified water. The resulting precipitate was collected by filtration and washed with distilled water, then air-dried. The crude product was then recrystallized from methanol to give **3a**. Yield 2.85 g (84%) as a white crystalline solid, mp 181 °C. Anal. calcd. for $C_{20}H_{19}ClN_2O$: C, 70.90; H, 5.65; N, 8.27%. Found: C, 70.78; H, 5.58; N, 8.59. IR (KBr): ν, cm^{-1}

2233 (CN). ^{1}H NMR (400 MHz, $CDCl_3$, 25 °C): δ, ppm 1.14 (d, 6H, 2-CH_3), 1.22 (d, 6H, 2-CH_3), 2.75 (sept, 2H, 2-CH_3CHCH_3), 6.76 (s, 1H, Pc Ar-H), 7.30 (d, 2H, Ar-H), 7.37 (t, 1H, Ar-H), 7.91 (s, 1H, Pc Ar-H). MS (EI): *m/z* 338 (calcd. for $[M]^+$ 338.5998].

2,9,16,23-tetrachloro-3,10,17,24-tetra(2,6-di-*iso*-propylphenoxy)phthalocyanine (4a). A solution of 4-chloro-5-(2,6-di-*iso*-propylphenoxy)phthalonitrile (**3a,** 1.00 g, 2.95 mmol), and urea (0.35 g, 6 mmol), in dry quinoline (10 mL) was heated at 180°C under nitrogen for 12 h. On cooling the reaction mixture was poured into 200 mL of stirred distilled water and neutralized with hydrochloric acid. The resulting solid product was collected by filtration, washed with water and methanol. The crude product was purified by column chromatography on silica (eluent DCM) to give **4a**. Yield 0.28 g (28%) as a greenish-blue powder, mp > 300 °C. Anal. calcd. for $C_{80}H_{78}Cl_4N_8O_4$: C, 70.79 H, 5.79; N, 8.26%. Found: C, 71.18; H, 5.53; N, 7.95. IR (KBr): ν, cm^{-1} 3964 (Ar-H), 1607 (C=N). UV-vis (DMF): λ_{max}, nm (log ε) 668 (5.13), 703 (5.21). ^{1}H NMR (600 MHz, $CDCl_3$, 25 °C): δ, ppm -0.53 (s, 2H, -NH), 1.15–1.37 (m, 48H, 16-CH_3), 3.20–4.24 (m, 8H, 4-CH_3CHCH_3), 7.45–9.51 (m, 20H, Pc Ar-H and Ar′-H). MS (FAB): *m/z* 1357 (calcd. for $[M]^+$ 1356.4259).

A general procedure for synthesis of complexes **5a**–**8a** is as follows. A mixture of **3a** (1.00 g, 2.95 mmol) and excess of anhydrous metal salt (40 mg) in dry quinoline (5 mL) and few drops of DBU was stirred at 180 °C under nitrogen for 12 h. The reaction mixture was poured into stirred distilled water (200 mL) on cooling, and the solid product was collected by filtration, washed with water and methanol. The crude product was purified by column chromatography on silica using the appropriate eluent as stated for each complex below.

2,9,16,23-tetrachloro-3,10,17,24-tetra(2,6-di-*iso*-propylphenoxy)phthalocyaninatozinc (5a). Zinc acetate used as metal salt. Eluent used: hexane-DCM (1:1) to give **5a**. Yield 0.20 g (19%) as a greenish-blue powder, mp > 300 °C. Anal. calcd. for $C_{80}H_{76}Cl_4N_8O_4Zn$: C, 67.63; H, 5.39; N, 7.88%. Found: C, 67.37; H, 5.49; N, 7.54. IR (KBr): ν, cm^{-1} 3962 (Ar-H), 1605 (C=N). UV-vis (DMF): λ_{max}, nm (log ε) 680 (5.35). ^{1}H NMR (600 MHz, $CDCl_3$, 25 °C): δ, ppm 1.10–1.60 (m, 48H, 16-CH_3), 3.21–4.21 (m, 8H, 4-CH_3CHCH_3), 7.39–9.05 (m, 20H, Pc Ar-H and Ar′-H). MS (FAB): *m/z* 1417 (calcd. for $[M]^+$ 1419.7903).

2,9,16,23-tetrachloro-3,10,17,24-tetra(2,6-di-*iso*-propylphenoxy)phthalocyaninatoaluminum chloride (6a). Aluminum chloride used as metal salt. Eluent used: ethyl acetate-THF (4:1) to give **6a**. Yield 0.29 g (28%) as a green powder, mp > 300 °C. Anal. calcd. for $C_{80}H_{76}Cl_5N_8O_4Al$: C, 67.77; H, 5.40; N, 7.90%. Found: C, 67.45; H, 5.87; N, 7.65. IR (KBr): ν, cm^{-1} 3963 (Ar-H), 1607 (C=N). UV-vis (DMF): λ_{max}, nm (log ε) 683 (5.29). ^{1}H NMR (600 MHz, $CDCl_3$, 25 °C): δ, ppm 1.07–1.45 (m, 48H, 16-CH_3), 3.14–3.45 (m, 8H, 4-CH_3CHCH_3), 7.46–9.63 (m, 20H, Pc Ar-H and Ar′-H). MS (FAB): *m/z* 1417 (calcd. for $[M]^+$ 1416.6608).

2,9,16,23-tetrachloro-3,10,17,24-tetra(2,6-di-*iso*-propylphenoxy)phthalocyaninatogallium chloride (7a). Gallium chloride used as metal salt. Eluent used: DCM-ethyl acetate (4:1) to give **7a**. Yield 0.19 g (17.5%) as a green powder, mp > 300 °C. Anal. calcd. for $C_{80}H_{76}Cl_5N_8O_4Ga$: C, 65.79; H, 5.25; N, 7.67%. Found: C, 65.41; H, 5.36; N, 7.39. IR (KBr): ν, cm^{-1} 3963 (Ar-H), 1606 (C=N). UV-vis (DMF): λ_{max}, nm (log ε) 688 (5.27). ^{1}H NMR (600 MHz, $CDCl_3$, 25 °C): δ, ppm 1.04–1.80 (m, 48H, 16-CH_3), 3.21–4.25 (m, 8H, 4-CH_3CHCH_3), 7.43–9.71 (m, 20H, Pc Ar-H and Ar′-H). MS (FAB): *m/z* 1460 (calcd. for $[M]^+$ 1459.5859).

2,9,16,23-tetrachloro-3,10,17,24-tetra(2,6-di-*iso*-propylphenoxy)phthalocyaninatoindium chloride (8a). Indium chloride used as metal salt. Eluent used: hexane-DCM (1:5) to give **8a**. Yield 0.25 g (22.5%) as a green powder, mp > 300 °C. Anal. calcd. for $C_{80}H_{76}Cl_5N_8O_4In$: C, 63.82; H, 5.09; N, 7.44%. Found: C, 64.22; H, 5.27; N, 7.54. IR (KBr): ν, cm^{-1} 3964 (Ar-H), 1605 (C=N). UV-vis (DMF): λ_{max}, nm (log ε) 693 (5.21). ^{1}H NMR (600 MHz, $CDCl_3$, 25 °C): δ, ppm 0.94–1.46 (m, 48H, 16-CH_3), 3.02–3.39 (m, 8H, 4-CH_3CHCH_3), 7.42–9.65 (m, 20H, Pc Ar-H and Ar′-H). MS (FAB): *m/z* 1505 (calcd. for $[M]^+$ 1504.6809).

4,5-bis-(2,6-di-*iso*-propylphenoxy)phthalonitrile (3b) [20]. Dry potassium carbonate (30.00 g, 217 mmol) was added to a solution of 4,5-dichlorophthalonitrile (**1**, 10.0 g, 50.7 mmol) and 2,6-di-*iso*-propylphenol (**2**, 22.25 g, 125.0 mmol) in dry dimethylformamide and were reacted according to the procedure used for **3a** to give the crude compound which was purified by recrystallization from methanol to give **3b**. Yield 18.3 g (75%) as a white solid, mp 161–163 °C. Anal. calcd. for $C_{32}H_{36}N_2O_2$: C, 79.95; H, 7.50; N, 5.83%. Found: C, 79.91; H, 7.60; N, 5.80. IR (KBr): ν, cm^{-1} 3082, 2228, 1590, 1500, 1342, 1096, 880, 795. ^{1}H NMR (400 MHz; $CDCl_3$): δ, ppm 7.25 (m, 6H, Ar-H), 6.70 (s, 2H, Pc Ar-H), 2.88 (sept, 4H, J = 6.7 Hz, CH_3CHCH_3), 1.20 (d, 12H, J = 6.7 Hz, CH_3CHCH_3), 1.10 (d, 12H, J = 6.7 Hz, CH_3CHCH_3). MS (EI): *m/z* 480 (calcd. for $[M]^+$ 480.2778).

2,3,9,10,16,17,23,24-octa(2,6-di-*iso*-propylphenoxy)phthalocyaninato (4b) [20]. To a solution of 4,5-bis(2,6-di-*iso*-propylphenoxy)phthalonitrile (**3b**, 0.20 g, 0.42 mmol), in refluxing anhydrous 1-pentanol (3 mL) and under nitrogen, an excess of lithium was added. The reaction mixture was refluxed for 5 h and then cooled and acetic acid added (1 mL, 0.1 M). The solvent was removed under reduced pressure to give the crude product. Purification by column chromatography on SiO_2, eluting with DCM to give **4b**. Yield 0.08 g (40%) as a green solid, mp > 300 °C. Anal. calcd. for $C_{128}H_{146}N_8O_8$: C, 79.88; H, 7.65; N, 5.82%. Found: C, 80.04; H, 7.70; N, 5.70. IR (film): ν, cm^{-1} 3576, 2962, 1439, 1328, 1265, 1184, 1093, 1017, 877, 754. UV-vis (DMF): λ_{max}, nm (log ε) 701 (5.30). ^{1}H NMR (400 MHz,

$CDCl_3$): δ, ppm 8.13 (br, 8H, Pc Ar-H), 7.50 (m, 24H, Ar-H), 3.37 (sept, 16H, *J* = 6.5 Hz, CH_3CHCH_3), 1.28 (br m, 96H, CH_3CHCH_3), -0.84 (s, 2H, -NH). MS (FAB): *m/z* 1925.71 (calcd. for $[M]^+$ 1923.1272).

2,3,9,10,16,17,23,24-octa(2,6-di-*iso*-propylphenoxy)phthalocyaninatozinc (5b) [20]. A stirred solution of 4,5-bis (2,6-di-*iso*-propylphenoxy)phthalonitrile (**3b**, 0.30 g, 0.6 mmol) and zinc(II) acetate (0.1 g, 0.6 mmol) in quinoline (1 mL) was heated at 180 °C for 12 h under nitrogen. The reaction mixture was cooled to room temperature and poured into methanol (15 mL). The crude product was purified by column chromatography on SiO_2, eluting with hexane-DCM (4:6) to give **5b**. Yield 0.2 g (67%) as a green solid, mp > 300 °C. Anal. calcd. for $C_{128}H_{144}N_8O_8Zn$: C, 77.59; H, 7.32; N, 5.66%. Found: C, 77.68; H, 7.52; N, 5.52. IR (film): ν, cm^{-1} 2961, 1612, 1456, 1462, 1413, 1353, 1269, 1186, 1095, 1050, 904, 864, 799, 777, 755, 729. UV-vis (DMF): λ_{max}, nm (log ε) 675 (5.57). ^1H NMR (400 MHz, $CDCl_3$): δ, ppm 8.17 (s, 8H, Pc Ar-H), 7.62 (t, 8H, *J* = 7.8 Hz, Ar-H), 7.5 (br s, 16H, Ar-H), 3.46 (br s, 16H, CH_3CHCH_3), 1.30 (br m, 96H, CH_3CHCH_3). MS (FAB): *m/z* 1988 (calcd. for $[M]^+$ 1986.4915).

Complexes **6b**–**8b** were synthesized and purified as outlined for **(5b)**.

2,3,9,10,16,17,23,24-octa(2,6-di-*iso*-propylphenoxy)phthalocyaninatoaluminum chloride (6b). Aluminum(III) chloride used as metal salt. Eluent used: hexane-DCM-ethyl acetate (4:4:1) to give **6b**. Yield 0.12 g (20%) as a green solid, mp > 300 °C. Anal. calcd. for $C_{128}H_{144}ClN_8O_8Al$: C, 77.48; H, 7.26; N, 5.65%]. Found: C, 77.52; H, 7.45; N, 5.80. IR (film): ν, cm^{-1} 2962, 1621, 1463, 1414, 1354, 1330, 1272, 1185, 1093. UV-vis (DMF): λ_{max}, nm (log ε) 691 (5.48). ^1H NMR (400 MHz, $CDCl_3$): δ, ppm 8.22 (s, 8H, Pc Ar-H), 7.61 (t, 8H, *J* = 7.8 Hz, Ar-H), 7.50 (br s, 16H, Ar-H), 3.43 (br s, 16H, CH_3CHCH_3), 1.27 (br m, 96H, CH_3CHCH_3). MS (FAB): *m/z* 1982 (calcd. for $[M]^+$ 1983.5457).

2,3,9,10,16,17,23,24-octa(2,6-di-*iso*-propylphenoxy)phthalocyaninatogallium chloride (7b). Gallium(III) chloride used as metal salt. Eluent used: DCM to give **7b**. Yield 0.04 g (40%) as a green solid, mp > 300 °C. Anal. calcd. for $C_{128}H_{144}ClGaN_8O_8$: C, 75.85; H, 7.11; N, 5.53%. Found: C, 75.60; H, 7.98; N, 5.78. IR (film): ν, cm^{-1} 2963, 1610, 1452, 1400, 1265, 1185, 1090. UV-vis (DMF): λ_{max}, nm (log ε) 690 (5.43). ^1H NMR (400 MHz, $CDCl_3$): δ, ppm 8.19 (s, 8H, Pc Ar-H), 7.60 (t, 8H, *J* = 7.6 Hz, Ar-H), 7.48 (r s, 16H, Ar-H), 3.41 (br s, 16H, CH_3CHCH_3), 1.33 (br m, 96H, CH_3CHCH_3). MS (FAB): *m/z* 2025 (calcd. for $[M]^+$ 2026.2872).

2,3,9,10,16,17,23,24-octa(2,6-di-*iso*-propylphenoxy)phthalocyaninatoindium chloride (8b). Indium(III) chloride was used as metal salt. Eluent used: DCM to give **8b**. Yield 0.03 g (38%) as a green solid, mp > 300 °C. Anal. calcd. for $C_{128}H_{144}ClInN_8O_8$: C, 74.17; H, 7.00; N, 5.41%. Found: C, 73.62; H, 7.36; N, 4.93. IR (film): ν, cm^{-1} 2965, 1617, 1461, 1410, 1280, 1182, 1090. UV-vis (DMF): λ_{max}, nm (log ε) 690 (5.38). ^1H NMR (400 MHz, $CDCl_3$): δ, ppm 8.17 (s, 8H, Pc Ar-H), 7.61 (t, 8H, *J* = 7.6 Hz, Ar-H), 7.52 (br s, 16H, Ar-H), 3.35 (br s, 16H, CH_3CHCH_3), 1.28 (br m, 96H, CH_3CHCH_3). MS (FAB): *m/z* 2072 (calcd. for $[M]^+$ 2071.3822).

CONCLUSION

The synthesis of novel metal free, zinc, aluminum, gallium and indium phthalocyanines terminated by four or eight di-*iso*-propylphenoxy groups has been reported. Supporting characterization techniques confirm the predicted structural configuration of these molecules. It was found that the steric factor produced by the peripheral substituents play a major role in perfectly preventing, the common aggregation behavior of Pc complexes as confirmed by ^1H NMR and UV-vis spectroscopic techniques. Consequently the effects of substituents (*i.e.* phenoxy or chlorine atoms) or the central metals on the physicochemical properties have been investigated. Low fluorescence quantum yields were accompanied by large triplet quantum yields, particularly for the tetra-substituted species. Considering the central metal atom, an increase in the size of the central metal atom yielded a similar effect in response to the heavy atom effect. Fluorescence lifetimes fall within the range typical of phthalocyanines, with the aluminum species (**6a** and **6b**) showing extended lifetimes in the S_1 state relative to the other Pc derivatives. All phthalocyanine derivatives in this study generally produced singlet oxygen with relatively good quantum yields. The photophysicochemical properties determined thus suggest that these molecules may be considered for either PDT or optical limiting applications.

Acknowledgements

AT wishes to thank the College of Graduate Studies, Kuwait University for a Ph.D. candidacy. The financial support of ANALAB and SAF grants (Nos. GS 01/01, GS 01/05 and GS 03/01), Kuwait University, and the support by the Department of Science and Technology (DST) and National Research Foundation (NRF), South Africa through DST/NRF Chairs Initiative for Professor of Medicinal Chemistry and Nanotechnology and Rhodes University are gratefully acknowledged. WC thanks Rhodes University for funding.

REFERENCES

1. Gregory P. *J. Porphyrins Phthalocyanines* 2000; **4**: 432–437.
2. Okura I. *Photosensitization of Porphyrins and Phthalocyanines*, Gordon and Breach Science Publishers: Amsteldijk, the Netherlands, 2001.
3. Ben-Hur E, Green M, Prager A, Kol R and Rosenthal I. *Photochem. Photobiol.* 1987; **46**: 651–656.
4. Nalwa HS and Shirk JS. In *Nonlinear Optical Properties of Metallophthalocyanines*. In *Phthalocyanines:*

Properties and Applications, Vol. 1, Leznoff CC and Lever ABP. (Eds.) VCH Publishers: New York, 1989; pp 83–172.
5. Chen Y, Hanack M, Blau WJ, Dini D, Liu Y, Lin and Bai J. *J. Mater. Sci*. 2006; **41**: 2169–2185.
6. Ma L, Zhang Y and Yuan P. *Opt. Express* 2010; **18**: 17666–17671.
7. Shirk JS, Lindle JR, Bartoli FJ, Kafafi ZH and Snow AW. *Mater. Nonlinear Opt.* 1991; **455**: 626–634.
8. De la Torre G, Vázquez P, Agulló-López F and Torres T. *J. Mater. Chem.* 1998; **8**: 1671–1683.
9. Tedesco AC, Rotta JCG and Lunardi CN. *Curr. Org. Chem.* 2007; **3**: 187–196.
10. Guo L, Meng FS, Gong XD, Xiao HM, Chen KC and Tian H. *Dyes Pigm.* 2001; **49**: 83–91.
11. Nyokong T and Antunes E. In *Photochemical and Photophysical Properties of Metallophthalocyanines*. *The Handbook of Porphyrin Science*, Vol. 7, Kadish KM, Smith KM and Guilard R. (Eds.) World Scientific: Singapore, 2010; pp 247–358.
12. Erdogmus A and Nyokong T. *Polyhedron* 2009; **28**: 2855–2862.
13. Lo P-C, Leng X and Ng DKP. *Coord. Chem. Rev.* 2007; **251**: 2334–2353.
14. Rodríguez-Morgade MS, de la Torre G and Torres T. In *Design and Synthesis of Low-Symmetry Phthalocyanines and Related Systems*, *The Porphyrin Handbook*, Vol. 15, Kadish KM, Smith KM and Guilard R. (Eds.) Academic Press: New York, 2003; pp 125–155.
15. Banfi S, Carous E and Buccafurni L. *J. Organomet. Chem.* 2007; **692**: 1269–1276.
16. Kluson P, Drobek M, Kalaji A, Zarubova S, Krysa J and Rakusan J. *J. Photochem. Photobiol. A* 2008; **199**: 267–273.
17. Yslas EI, Rivarola V and Durantini EN. *Bioorg. Med. Chem.* 2005; **15**: 39–46.
18. Yslas EI, Durantini EN and Rivarola V. *Bioorg. Med. Chem.* 2007; **15**: 4651–4660.
19. Oda K, Ogura SI and Okura I. *J. Photochem. Photobiol. B* 2000; **59**: 20–25.
20. Makhseed S and Samuel J. *Dyes Pigm.* 2009; **82**: 1–5.
21. McKeown NB, Makseed S, Msayib KJ, Ooi LL, Helliwell M and Warren JE. *Angew. Chem.* 2005; **117**: 7718–7721.
22. Lo PC, Wang S, Zeug A, Meyer M, Röder B and Ng DKP. *Tetrahedron Lett.* 2003; **44**: 1967–1970.
23. Lo PC, Chan CMH, Liu JY, Fong WP and Ng DKP. *J. Med. Chem.* 2007; **5**: 2100–2107.
24. Siejak A, Wróbel D and Ion RM. *J. Photochem. Photobiol. A* 2006; **181**: 180–187.
25. Musil Z, Zimcik P, Miletin M, Kopecky K, Petrik P and Lenco J. *J. Photochem. Photobiol.* 2007; **186**: 316–322.
26. Wöhrle D, Eskes M, Shigehara K and Yamada A. *Synthesis* 1993; 194–196.
27. Shirk JS, Pong RGS, Flom SR, Heckmann H and Hanack M. *J. Phys. Chem. A* 2000; **104**: 1438–1449.
28. Dini D, Barthel M and Hanack M. *Eur. J. Org. Chem.* 2001; 3759–3769.
29. Macdonald IJ and Dougherty TJ. *J Porphyrins Phthalocyanines* 2001; **5**: 105–129.
30. Xu TH, Xie WW, Guo CY, Ci Y, Chen JL and Peng JXB. *J. Chin. Chem. Soc*. 2007; **54**: 211–217.
31. Law WF, Liu KM and Ng DKP. *J. Mater. Chem.* 1997; **7**: 2063–2067.
32. Tai S and Hayashi N. *J. Chem. Soc. Perkin Trans. 2* 1991; 1275–1279.
33. Choi MTM, Li PPS and Ng DKP. *Tetrahedron* 2000; **56**: 3881–3887.
34. Sergeyev S, Pouzet E, Debever O, Levin J, Gierschner J, Coornil J, Gomez-Aspe R and Geerts YH. *J. Mater. Chem.* 2007; **17**: 1777–1784.
35. Cook MJ and Jafari-Fini A. *J. Mater. Chem.* 1997; **7**: 2327–2329.
36. Barthel M, Dini D, Vagin S and Hanack M. *Eur. J. Org. Chem.* 2002; **2**: 3756–3762.
37. Patonay G, Antoine MD, Devanathan S and Strekowski L. *Appl. Spectrosc.* 1991; **45**: 457–461.
38. Stillman MJ and Nyokong T. In *Synthesis, Spectroscopic and Electrochemical Properties of Phthalocyanines*. *Phthalocyanines: Properties and Applications*, Vol. 1, Leznoff CC and Lever ABP. (Eds.) VCH Publishers: New York, 1989; Chapter 3, pp 139–247.
39. Shinohara H, Tsaryova, O, Schnurpfeil G and Wöhrle D. *J. Photochem. Photobiol. A* 2000; **18**: 50–57.
40. Huang JD, Wang S, Lo PC, Fong WP, Ko WH and Ng DKP. *New. J. Chem.* 2004; **28**: 348–354.
41. Senge MO. *Chem. Commun.* 2006; 243–256.
42. Lakowicz JR. *Principles of Fluorescence Spectroscopy* (2nd ed.), Kluwer Academic/Plenum Publishers: New York, 1999.
43. Owens JW, Smith R, Robinson R and Robins M. *Inorg. Chim. Acta* 1998; **279**: 226–231.
44. Owens JW and Robins M. *J. Porphyrins Phthalocyanines* 2001; **5**: 460–464.
45. Ermilov EA, Tannert S, Werncke T, Choi MTM, Ng DKP and Röder B. *Chem. Phys.* 2006; **328**: 428–437.
46. Idowu M and Nyokong T. *J. Luminescence* 2009; **129**: 356–362.
47. Ogunsipe A and Nyokong T. *J. Photochem. Photobiol. A* 2005; **17**: 211–220.
48. Ogunsipe A and Nyokong T. *Photochem. Photobiol. Sci.* 2005; **4**: 510–516.
49. Turro NJ. *Modern Molecular Photochemistry*, The Benjamin/Cummings Publishing Co. Inc: California, 1978.
50. Kobayashi N, Mack J, Ishii K and Stillman MJ. *Inorg. Chem.* 2002; **41**: 5350–5363.
51. Chidawanyika W and Nyokong T. *J. Photochem. Photobiol. A* 2009; **206**: 169–176.

52. Perrin DD and Amarego LF. *Purification of Laboratory Chemicals* (2nd ed.), Pergamon Press: Oxford, 1989.
53. Fery-Forgues S and Lavabre D. *J. Chem. Educ.* 1999; **76**: 1260–1264.
54. Fu J, Li XY, Ng DKP and Wu C. *Langmuir* 2002; **18**: 3843–3847.
55. Tran-Thi TH, Desforge C and Thiec C. *J. Phys. Chem.* 1989; **93**: 1226–1233.
56. Kossanyi J and Chahraoui D. *Int. J. Photoenergy* 2000; **2**: 9–15.
57. Spiller W, Kliesch H, Wöhrle D, Hackbarth S, Röder B and Schnurpfeil G. *J. Porphyrins Phthalocyanines* 1998; **2**: 145–158.
58. Ogunsipe A, Chen JY and Nyokong T. *New. J. Chem.* 2004; **28**: 822–827.